Supporting Experimental Procedure

Neuroligin3 splice isoforms shape inhibitory synaptic function in the mouse hippocampus

Motokazu Uchigashima[1,2,5], Ming Leung[3,5], Takuya Watanabe[1,5], Amy Cheung[1], Timmy Le[1], Sabine Pallat[1], Alexandre Luis Marques Dinis[1], Masahiko Watanabe[2], Yuka Imamura Kawasawa[3,4*] and Kensuke Futai[1*]

[1]Brudnick Neuropsychiatric Research Institute, Department of Neurobiology, University of Massachusetts Medical School, 364 Plantation Street, LRB-706 Worcester, MA 01605-2324, USA
[2]Department of Anatomy, Hokkaido University Graduate School of Medicine, Sapporo, Hokkaido 060-8638, Japan
[3]Department of Biochemistry and Molecular Biology and Institute for Personalized Medicine, Pennsylvania State University College of Medicine, 500 University Drive, Hershey, Pennsylvania 17033, USA
[4]Department of Pharmacology Pennsylvania State University College of Medicine, 500 University Drive, Hershey, Pennsylvania 17033, USA
[5]These authors contributed equally

*Corresponding authors:
Yuka Imamura Kawasawa
E-mail: yimamura@pennstatehealth.psu.edu
Kensuke Futai
E-mail: Kensuke.Futai@umassmed.edu

Plasmid constructs: The expression vector for HA-tagged mouse *Nlgn3Δ* has been reported previously (11). Three HA-tagged *Nlgn3* splice variants, *Nlgn3A1, Nlgn3A2* and *Nlgn3A1A2*, were cloned to pCAG vector using a PCR-based method.

Single-cell sequencing and analysis: *Single-Cell RNA Extraction:* The whole cell patch-clamp technique was used to harvest single cell cytosol (6). Briefly, glass electrodes (1.5 – 2.0 MΩ) were filled with DEPC-treated internal solution containing (in mM): 140 K-methanesulfonate, 0.2 EGTA, 2 $MgCl_2$ and 10 HEPES, pH-adjusted to 7.3 with KOH. RNase inhibitor (1 U/µl, Ambion) was included in the internal solution. Immediately after establishing whole-cell mode, the cytosol of the recorded cell was aspirated into the patch pipette and immediately expelled into an RNase-free 0.5-ml tube (Ambion). *Library Preparation and mRNA Sequencing:* The cDNA libraries were prepared using a SMART-Seq® HT Kit (TAKARA Bio) and a Nextera XT DNA Library Prep Kit (Illumina) as per the manufacturers' instructions. Unique barcode sequences were incorporated into the adaptors for multiplexed high-throughput sequencing. The final product was assessed for its size distribution and concentration using a BioAnalyzer High Sensitivity DNA Kit (Agilent Technologies). The libraries were pooled and diluted to 3 nM using 10 mM Tris-HCl (pH 8.5) and then denatured using the Illumina protocol. The denatured libraries were loaded onto an S1 flow cell on an Illumina NovaSeq 6000 (Illumina) and run for 2 x 50 cycles according to the manufacturer's instructions. De-multiplexed sequencing reads were generated using Illumina bcl2fastq (version 2.18.0.12) allowing no mismatches in the index read. *Data Analysis*: BBDuk (https://jgi.doe.gov/data-and-tools/bbtools/bb-tools-user-guide/bbduk-guide/) was used to trim/filter low quality sequences using the "qtrim=lr trimq=10 maq=10" option. Next, alignment of the filtered reads to the mouse reference genome (GRCm38) was performed using HISAT2 (version 2.1.0) (https://genomebiology.biomedcentral.com/articles/10.1186/gb-2013-14-4-r36) applying --no-mixed and --no-discordant options. Read counts were calculated using HTSeq (http://bioinformatics.oxfordjournals.org/content/31/2/166) by supplementing Ensembl gene annotation (GRCm38.78). Gene expression values were calculated as transcripts per million (TPM) using custom R scripts. Genes with no detected TPM in all samples were filtered out. The log2+1 transformed TPM values were combined with "Cell Diversity in the Mouse Cortex and Hippocampus RNA-Seq Data" from the Allen Institute for Brain Science (https://portal.brain-map.org/atlases-and-data/rnaseq#Mouse_Cortex_and_Hip) where large-scale single-cell RNA-seq data were collected from the adult mouse brain. RNA sequencing data were generated from single cells isolated from >20 areas of the mouse cortex and hippocampus, including ACA, AI, AUD, CA, CLA, CLA;EPd, ENTl, ENTm, GU;VISC;AIp, HIP, MOp, MOs, ORB, PAR;POST;PRE, PL;ILA, PTLp, RSP, RSPv, SSp, SSs, SSs;GU, SSs;GU;VISC, SUB;ProS, TEa;PERI;ECT, VISal;VISl;VISli, VISam;VISpm, VISp and VISpl;VISpor (abbreviations for each cell type match those found in the Allen Mouse Brain Atlas (https://portal.brain-map.org/explore/classes/nomenclature)). The provided table of median expression values for each gene in each cell type cluster was merged with our data, and a tSNE plot was generated using Rtsne R package (29). For splice isoform quantification, kallisto (30) was used by supplementing the transcript fasta file (Mus_musculus.GRCm38.cdna.all.fa), which was manually modified to include six *Nlgn* splice isoforms (*Nlgn1A*_XM_006535423.3, *1B*_XM_006535424.4, *2Δ*_XM_006532902.4, *2A*_XM_006532903.3, *3Δ* and *3A1*) that were not annotated by the Mus_musculus.GRCm38.cdna.all.fa dataset. The manually curated transcript sequences are provided in **Fig. S2**.

Single-cell semi-quantitative RT-PCR (semi-RT-qPCR): The single cell cytosol was harvested using the whole cell patch-clamp technique as described earlier and the cDNA was prepared using a SMART-Seq® HT Kit (TAKARA Bio) as per the manufacturers' instructions. The semi-quantitative PCR was performed using GoTaq Master Mix (Promega) and primers for *Nlgn1*, *Nlgn2* and *Nlgn3* splice variants are: NL1, 5'-CTATACTTAAACATCTATGTCCCA -3' and 5'- GCTGGAAAGGGCTGTTCCACTCTGA -3'; NL2A, 5'- CTGTACCTCAACCTCTAC GTGCCC -3' and 5'- ATAGGCAGCCAGGACTGAGCCGTC -3'; NL3A1A2, 5'- CTCTATCTGAATGTGTATGTGCCC -3' and 5'-GTAACTTGCAAGAACACTGCCATCAAT -3'. The expected size of *Nlgn* splice isoforms are: *Nlgn1Δ*

(420 bp), *Nlgn1A* (480), *Nlgn1B* (447), *Nlgn1AB* (507), *Nlgn2Δ* (138), *Nlgn2A* (189), *Nlgn3Δ* (138), *Nlgn3A1* (198), *Nlgn3A2* (198), *Nlgn3A1A2* (258). The PCR product was assessed for its size and concentration using a BioAnalyzer High Sensitivity DNA Kit (Agilent Technologies).

Analysis of immunocytochemistry images: For quantification of HA signals, the peak signal intensity was measured at a pair of excitatory and inhibitory synapses on dendritic segments which were identified as a EGFP-labeled spine and its neighboring VIAAT-labeled inhibitory terminal, respectively. E-I balance ratio was calculated by dividing the peak signal intensity at excitatory synapses by that at inhibitory synapses. The background signal was determined as the mean signal intensity in EGFP-unlabeled regions, and then subtracted from the raw value to obtain the peak signal intensity. To assess the labeling intensity for VIAAT, the contour of VIAAT+ terminals was determined using binary images for the VIAAT channel. The mean intensity was measured in VIAAT+ terminals contacting and not contacting EGFP-labeled dendrites, and then normalized with the average intensity for VIAAT+ terminals which were not in contact with EGFP-labeled dendrites on the same image. This measurement was also applied to the labeling intensity for VGluT1. To assess the density of excitatory and inhibitory synapses, the number of spines and VIAAT+ inhibitory synapses were counted on individual dendritic segments, respectively. The mean length of dendritic segments was 19.7 ± 3.8, 21 ± 2.1, and 27.7 μm for CA1 pyramidal cells overexpressing HA-NLGN3Δ, 3A1A2, and EGFP control, respectively.

Electrophysiology: The extracellular solution consisted of (in mM): 119 NaCl, 2.5 KCl, 4 $CaCl_2$, 4 $MgCl_2$, 26 $NaHCO_3$, 1 NaH_2PO4, 11 glucose and 0.01 2-chloroadenosine (Sigma) gassed with 5% CO_2 and 95% O_2, pH of 7.4. Thick-walled borosilicate glass pipettes were pulled to a resistance of 2.5 – 4.0 MΩ. Whole-cell voltage-clamp recordings were performed with internal solution containing (in mM): 115 cesium methanesulfonate, 20 CsCl, 10 HEPES, 2.5 $MgCl_2$, 4 ATP disodium salt, 0.4 guanosine triphosphate trisodium salt, 10 sodium phosphocreatine and 0.6 EGTA, at pH 7.25 adjusted with CsOH. For current-clamp recordings, cesium was replaced by potassium. All experiments and the analysis of data were performed in a blind manner. Recordings were performed using a MultiClamp 700B amplifier and Digidata 1440, digitized at 10 kHz and filtered at 4 kHz using a low-pass filter. Data were acquired and analyzed using pClamp (Molecular Devices).

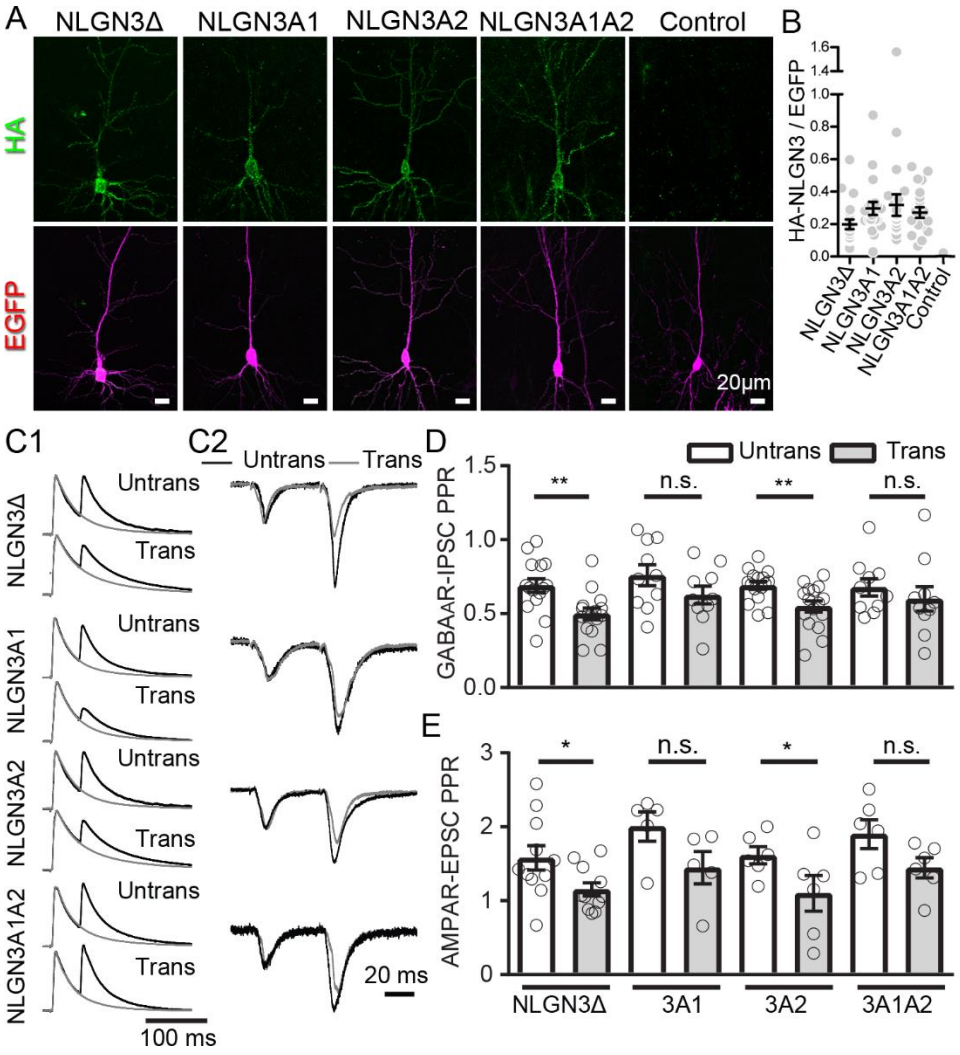

Figure S1. NLGN3 splice isoforms differentially regulate presynaptic release probability. Effect of NLGN3 splice isoform overexpression on gross morphology and PPR in hippocampal CA1 pyramidal cells. **A.** Low magnification images of entire neurons labeled with HA-NLGN3 and EGFP in CA1 pyramidal cells. **B.** Summary scatter plot showing the normalized intensity of HA signals in the cell bodies indicates that all four splice isoforms are equally overexpressed. **C.** Normalized sample traces of PPR of $GABA_AR$-IPSC (left, **C1**) and AMPAR-EPSC (right, **C2**). IPSCs and EPSCs are normalized to the first amplitude. Because the first $GABA_AR$-IPSC overlaps with the second IPSC, to accurately measure the amplitude of the second IPSC, we 'cancelled' the first IPSC by subtracting the traces receiving a single pulse (gray) from those receiving a paired pulse (black), both normalized to the first response. **D, E.** Summary of effect of NLGN3 transfection on IPSC- (**D**) and EPSC-PPR (**E**). Each bar represents the average of ratios obtained from multiple pairs of transfected and untransfected neighboring neurons. Number of cell pairs: NLGN3Δ ($GABA_AR$-IPSCs/AMPAR-EPSCs: 15/11); NLGN3A1 (10/5); NLGN3A2 (15/6); NLGN3A1A2 (10/6). ** $p < 0.01$, * $p < 0.05$, ns, not significant. Student's t-test.

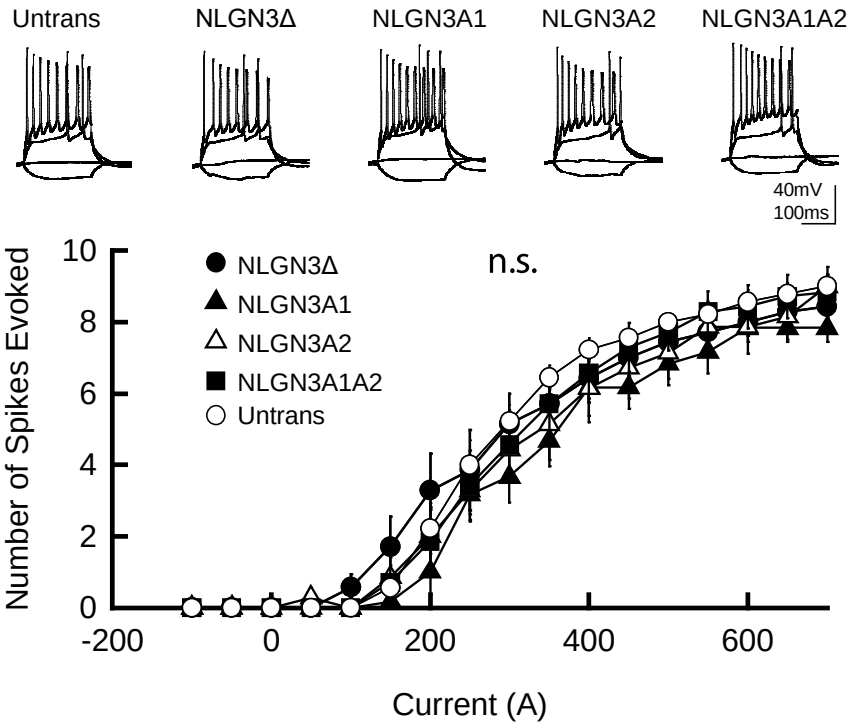

Figure S2. Membrane excitability is not altered by NLGN3 overexpression in CA1 pyramidal neurons. **Top.** Sample traces from untransfected and transfected CA1 pyramidal neurons in organotypic hippocampal slice cultures. The superimposed traces were elicited by current injections of -100, 0, 200 and 500 pA for 200 ms. **Bottom.** Summary graph of the frequency of action potentials in untransfected and transfected neurons. I-O relationship (number of spikes elicited vs. amount of current injection over a 200 ms duration) was plotted for untransfected and transfected neurons. Neurons were held at resting membrane potential (Rmv) and the I-O relationships were not significant between untransfected control and NLGN3 transfected neurons. Two-way ANOVA with *post hoc* Tukey. n.s.: not significant. Rmvs were not significant in five cell groups: untransfected, -58.9 ± 0.63; NLGN3Δ, -58.0 ± 0.52; NLGN3A1, -57.7 ± 0.37; NLGN3A2, -58.64 ± 0.81; NLGN3A1A2, -58.36 ± 0.70 mV. One-way ANOVA followed by Sidak's multiple comparisons test. Seven to nine cells from 2 mice were tested.

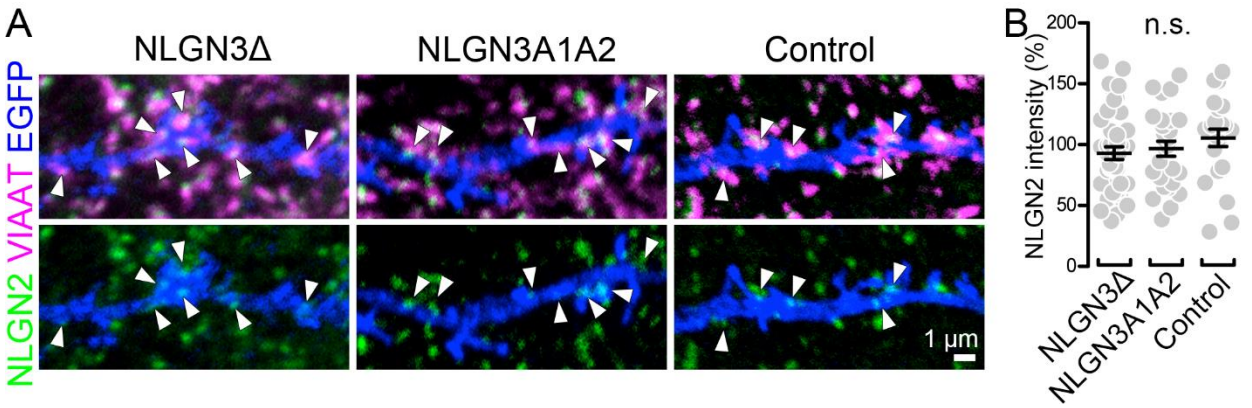

Figure S3. NLGN3 overexpression does not change synaptic targeting of NLGN2 in CA1 pyramidal neurons. **A.** Maximum projection images of dendritic segments labeled for NLGN2 (green), EGFP (blue) and VIAAT (magenta) in CA1 pyramidal cells overexpressing HA-NLGN3Δ (left), A1A2 (middle) and EGFP control (right). White arrow heads indicate VIAAT+ and NLGN2+ inhibitory synapses in transfected neurons. **B.** Summary scatter plot showing the normalized NLGN2 signals for individual VIAAT+ inhibitory synapses on the dendritic segment of CA1 pyramidal cells overexpressing HA-NLGN3Δ (left, n = 43 inhibitory synapses), A1A2 (middle, n = 27), and EGFP control (right, n = 23). Normalized NLGN2 intensity was obtained from neighboring VIAAT+ inhibitory synapses on the same image. n.s. not significant (one-way ANOVA followed by Sidak's multiple comparisons test).

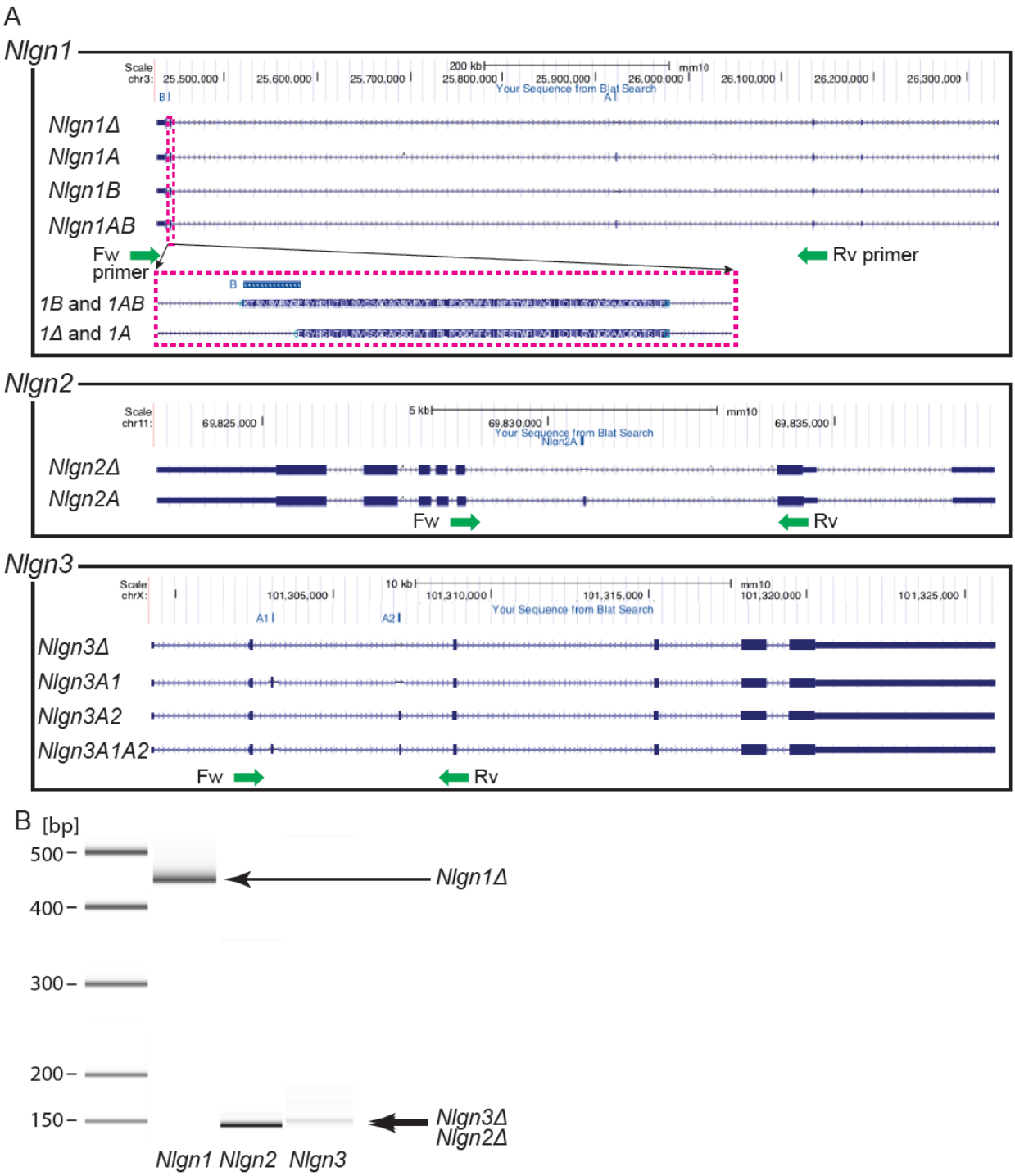

Figure S4. UCSC browser tracks of *Nlgn1, 2* and *3*, and semi-qPCR of hippocampal CA1 pyramidal neuron. **A.** 10 *Nlgn* transcripts and isoform-specific exons (A, B, *Nlgn*2A, A1 and A2; highlighted in blue) were manually curated. Green arrows depict locations of exon-specific PCR primers. **B.** Semi-quantitative RT-PCR of *Nlgn1*, *Nlgn2*, and *Nlgn3* in single-cell CA1 pyramidal neuron showed exclusive expression of Δ isoforms (predicted amplicon sizes for *Nlgn1Δ*=420 bp, *Nlgn2Δ*=138 bp, and *Nlgn3Δ*=138 bp).